

PHYSICAL REVIEW B

CONDENSED MATTER

THIRD SERIES, VOLUME 43, NUMBER 16 PART A

1 JUNE 1991

Channeling radiation and coherent bremsstrahlung for simple lattices: A three-dimensional approach

Sven-Erik Sandström* and Herbert Überall†

Department of Physics, Catholic University of America, Washington, D.C. 20064

(Received 15 October 1990)

The effect of the longitudinal variation of the lattice potential is investigated numerically for the case of electron channeling in the low-energy regime. Corrections to the energy of the emitted photons are found to be three dimensional (3D) rather than longitudinal, in character. These 3D effects are small and of about the same size as the error due to shortcomings in the description of the lattice potential. Coherent bremsstrahlung involves transitions between quantum states that emanate from the 3D nature of the potential. The corresponding photon energies and intensities are calculated and compared to available experimental results.

I. INTRODUCTION

Theoretical and experimental work on channeling radiation and coherent bremsstrahlung has been reported by many authors.¹ The more recent theoretical work involves the one- or two-dimensional (2D) Floquet-Bloch approach (planar or axial channeling), and is, to a large extent, due to Andersen and his co-workers.²⁻⁴

However, these studies of channeling radiation have used the transverse (or averaged, or projected, or continuum approximation) potential in the theoretical treatment. In an attempt to eliminate this approximation, Kurizki⁵ suggested a scheme that uses the transverse Floquet-Bloch modes in an iteration procedure intended to incorporate 3D effects without solving the 3D eigenvalue problem. The present paper is devoted to axial channeling and investigates the 3D problem, as well as a reduced eigenvalue problem that adds purely longitudinal modes to the transverse problem. Large eigenvalue problems require a substantial numerical effort and we have, therefore, employed the Lanczos algorithm^{6,7} in order to reduce computer time.

Coherent bremsstrahlung involves a low-intensity type of radiation that occurs in conjunction with channeling radiation but at higher photon energies. Spectra for this type of radiation have been obtained experimentally and described theoretically in terms of an essentially classical collision.⁸ Previous theoretical studies^{5,9} involve an admixture of classical and quantum-mechanical concepts and we have, therefore, relied squarely on quantum mechanics for the present treatment. The quantum ap-

proach is not suitable for the high-energy regime because of the prohibitively large numerical effort required. High energies tend to favor the use of classical techniques.¹

II. THEORY

If spin-dependent effects are neglected, one may take the linearized Klein-Gordon equation for the electron in the crystal potential as a starting point ($c = \hbar = 1$, $k_c^2 = E_c^2 - m^2$, $E_c \approx \gamma m$):

$$(\nabla^2 + k_c^2 - 2\gamma m V)\phi = 0. \quad (1)$$

The lattice potential can be expanded in a three-dimensional Fourier series in terms of the reciprocal-lattice vectors \mathbf{g} ,

$$V = \sum_{\mathbf{g}} U_{\mathbf{g}} e^{i\mathbf{g}\cdot\mathbf{x}}, \quad (2)$$

where the coefficients $U_{\mathbf{g}}$ contain the structure factor for the lattice, and the Doyle-Turner coefficients¹⁰ for the atomic potential. The standard Floquet-Bloch solution is written as

$$\phi = e^{i\mathbf{k}\cdot\mathbf{x}} \sum_{\mathbf{g}} C_{\mathbf{g}} e^{i\mathbf{g}\cdot\mathbf{x}}. \quad (3)$$

Combining these equations and projecting with respect to the basis yields the following eigenvalue problem:

$$\sum_{\mathbf{g}'} [(k_c^2 - k_{\parallel}^2 - D_{\mathbf{g}})\delta_{\mathbf{g}\mathbf{g}'} - 2\gamma m U_{\mathbf{g}-\mathbf{g}'}] C_{\mathbf{g}'} = 0, \quad (4)$$
$$D_{\mathbf{g}} = k_{\perp}^2 + 2\mathbf{k}\cdot\mathbf{g} + g^2.$$

The channeling axis is taken as the reference direction in \mathbf{k} space. Since we are primarily concerned with photon energies, we introduce the energy difference E (the quadratic term is a relativistic correction and can often be neglected; $E = E_c - \gamma m$):

$$\sum_{\mathbf{g}'} [(2\gamma m E + E^2 - D_{\mathbf{g}})\delta_{\mathbf{g}\mathbf{g}'} - 2\gamma m U_{\mathbf{g}-\mathbf{g}'}] C_{\mathbf{g}'} = 0. \quad (5)$$

A reduced eigenvalue problem is obtained by requiring \mathbf{g} and \mathbf{g}' to be either purely transverse or purely longitudinal, with respect to the channeling axis. The photon energy is given by the relation

$$E_{\gamma} = \frac{\Delta E}{1 - \beta \cos \theta}, \quad (6)$$

where ΔE and θ denote the transition energy and the polar angle of emission, respectively.

III. CHANNELING RADIATION

In order to study the axial, and essentially transverse, channeling problem, Eq. (5) was implemented numerically using the Lanczos algorithm.^{6,7} First, however, we would like to comment on the relationship between the iterative approach suggested by Kurizki,⁵ and the complete eigenvalue problem. We note that the iteration involves the solution of a dense linear system which requires a numerical effort comparable to that needed for an eigenvalue problem of the same size. This approach, therefore, implies a tradeoff between numerical effort, complexity of implementation, and approximation error. Numerical experiments indicate that the eigenvalue problem is sensitive to modification of matrix elements far from the main diagonal. Since the proposed iteration procedure⁵ involves partitioning of the problem into a transverse and a nontransverse part, with off-diagonal cross terms, it is unclear whether the iteration actually converges well enough for accurate eigenvalue calculations.

The transverse problem is a special case of Eq. (5). Figure 1 shows the transverse potential and the transverse energy levels for 4-MeV electrons along the $\langle 110 \rangle$ direction in silicon. The potential does not have the pronounced double well of the corresponding axis in diamond. The well is rather deep, however, thus requiring a large number of basis functions and the reduction in numerical effort provided by the Lanczos algorithm is, therefore, welcome. The splitting of the $2p$ state⁴ is moderate for this case, since the "molecular character" of the closest axes is less pronounced than in, for example, diamond. The "short-range" Doyle-Turner (DT) coefficients³ used in Fig. 1 were found to give a slightly larger splitting than the conventional DT coefficients. We have calculated the energy levels to five digits. The accuracy of the Doyle-Turner description of the potential^{11,12} may not warrant this precision but these numbers also serve as a reference for the convergence rate of the eigenvalue problem.

By varying the energy of the incident electron, we have verified that the Lindhard continuum approximation is good down to approximately 10 keV.¹³ Since traditional

TABLE I. Photon energies in the forward direction for 4-MeV electrons along the $\langle 110 \rangle$ direction.

Transverse	Silicon (eV)		3D
	Transverse	Transverse + longitudinal	
5947	5947	5940	
6023	6023	6016	
6585	6585	6577	

applications lie well above this limit, one could imagine that the 3D problem could be simplified by reducing the set of basis functions (rather than by attempting to solve the eigenvalue problem approximately). The question of whether a reduced set of basis functions can describe the details of channeling radiation is, thus, before us. Table I gives the photon energies for the transverse, reduced (i.e., transverse + longitudinal), and 3D case for 4-MeV electrons along the $\langle 110 \rangle$ direction in silicon. No correction for refraction has been made. We notice that the reduced formulation gives no shift at all. The reduced ansatz can be viewed as a "(2+1)-dimensional" solution where the one-dimensional part describes high-energy electrons traveling across lattice planes. Such an electron is essentially free and the effect of the "longitudinal lattice planes" is, therefore, negligible. As we can see in Table I, the 3D correction is rather small and seems to be at the

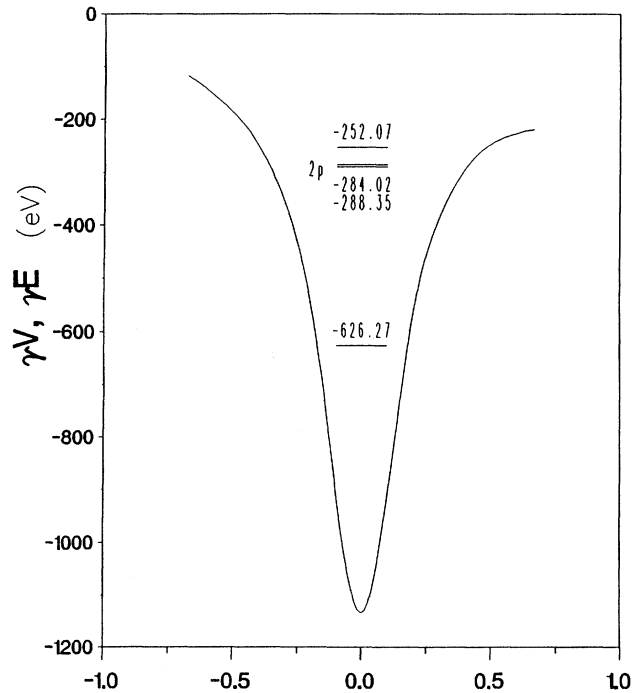


FIG. 1. Transverse potential and transverse energy levels for 4-MeV electrons along the $\langle 110 \rangle$ direction in silicon. 737 basis functions and a two-dimensional, mean-square, thermal displacement of 0.11 Å were used in the calculations. Half the double well is shown in order to obtain sufficient resolution.

overlap integral and makes a diffuse population more likely.

Table II presents the photon energies corresponding to Fig. 2 and Ref. 8. What we refer to as the classical results are obtained by letting $K_{\parallel}=0$ in Eq. (7). We notice that both the classical and the quantum-mechanical estimates are larger than the experimental values. The quantum results are corrected for refraction effects.^{1,2,4} For the quantum case, the discrepancy could be reduced somewhat by assuming that a number of transitions make up the peaks.¹⁸ This modification is, however, only adequate for the first peak; the others are too far off and too narrow to tally with such an explanation. The shifts produced by the transverse states are too small to suffice and whatever the population, there are no high-energy states with the desirable energies. One may argue that the change in relativistic mass caused by the transition should be accounted for. Neither of the states involved are affected to such an extent that the correction would be significant, however. It would seem reasonable that, when an electron loses a larger fraction of its energy, the transition would be more likely to involve inelastic and spin-dependent effects^{16,18} (or more exotic processes¹⁹). Consequently, theoretical estimates would be consistently larger than the experimental results. It is evident from Ref. 8, however, that the peaks also get sharper with increasing photon energy, thus contradicting the idea of a diffuse mechanism for energy loss. The linewidth corresponding to thermal scattering tends to increase with photon energy.¹⁸ Atomic excitations and plasmons are, in this context, essentially equivalent to small energy shifts (≈ 10 eV) in the band structure of the crystal and do not have the potential for any major interference with the emitted photon. Phonons, on the other hand, are important here because of their role in the transfer of momentum [cf. Eq. (7)] that governs the photon energy. The excitation of phonons with a well-defined dispersion relation¹⁷ could "stabilize the collision" and produce sharper peaks. Phonons could also account for some of the irregularity in other experimental data.⁹ While on this note, a mention of the moderate success of the theoretical description of positron channeling¹¹ is in order. For that case, the poor performance of the many-beam technique does not match up with the presumably small inelastic effects. All in all, however, the central role of lattice vibrations seems to call for more elaborate quantum-mechanical techniques. The poor accuracy of the many-beam formulation (cf., Table II) obviously also

TABLE II. Photon energies stemming from high-energy transitions radiating at an angle of 103° to the forward direction for 100-keV electrons along the $\langle 100 \rangle$ direction.

Classically	Diamond (keV)		Experiment
	Quantum mechanically		
1.67	1.61		1.61
3.32	3.39		3.20
4.93	5.12		4.80
6.51	6.85		6.30

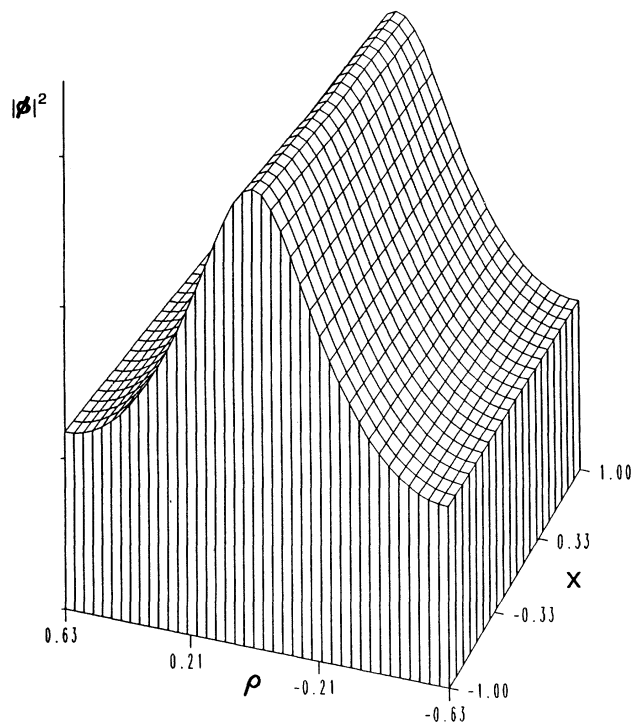


FIG. 3. Probability density for the ground state for 100-keV electrons along the $\langle 100 \rangle$ direction in diamond.

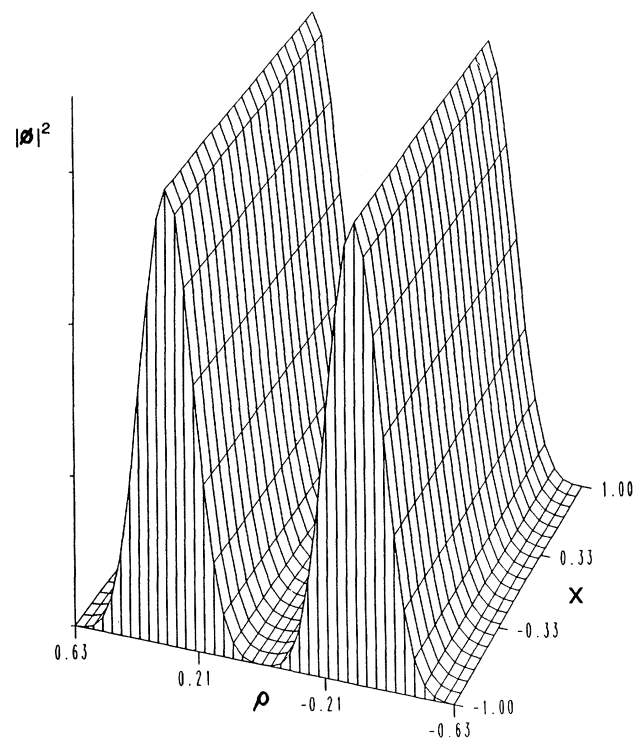


FIG. 4. Probability density for the first high-energy state for 100-keV electrons along the $\langle 100 \rangle$ direction in diamond.

has a bearing upon the various intensity formulas^{5,9,20} that rely on quantum states.

In order to obtain more insight into these transitions, we have calculated the probability densities for some of the states involved. Figure 3 shows the density for the ground state along the $\langle 100 \rangle$ direction in a plane containing nearest neighbors. This is, once again, the case of 100-keV electrons in diamond studied in Ref. 8. As one would expect, there is very little in the way of longitudinal variation. Figure 4 gives the corresponding density for the first "high-energy state" appearing in Fig. 2. The absence of any substantial longitudinal variation is less predictable for this state since it is truly three dimensional and does not exist in the transverse scenario. This also justifies the notion of a two-dimensional thermal vibration for these transitions. We notice that the transverse variation is consistent with the shift caused by the transverse projection of a short reciprocal-lattice vector. When compared to the corresponding low-energy channeling state given in Fig. 5, the difference in density profile is barely visible. The quantum-mechanical description of these high-energy transitions does, therefore, not reveal any new features that change our visualization of the electron's journey through the lattice.

The angular dependence of the intensity for coherent bremsstrahlung is given by the formula⁹

$$\frac{I}{I_{\max}} \propto \frac{1}{(1-\beta \cos\theta)^3} \left| \hat{\mathbf{q}}_r \times \sum_{\mathbf{g}} (\mathbf{k} + \mathbf{g}) C_{\mathbf{g}}^i C_{\mathbf{g}+\mathbf{G}}^{f*} \right|^2, \quad (11)$$

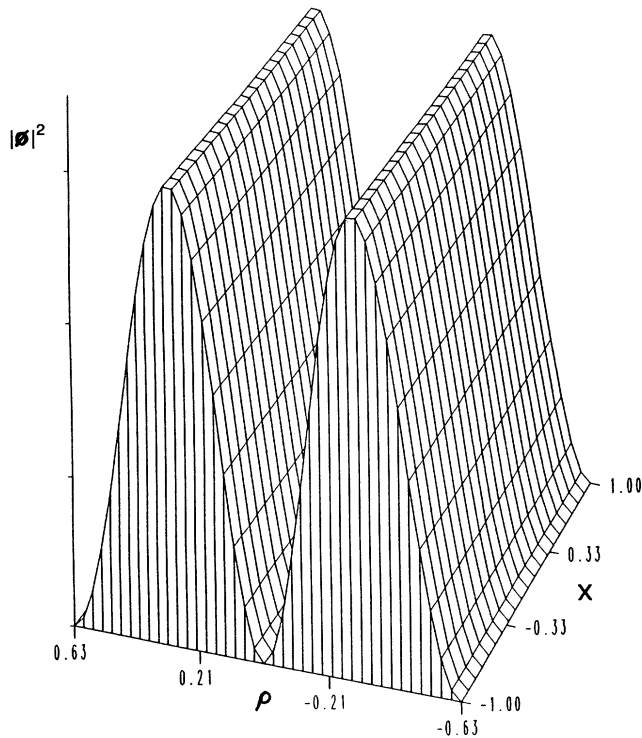


FIG. 5. Probability density for a channeling state with a transverse variation corresponding to that of the high-energy state discussed in conjunction with Fig. 4.

where $\hat{\mathbf{q}}_r$ is a unit vector in the rest frame direction of photon emission. The transformation of polar angles amounts to the relation

$$\cos\theta_r = \frac{1}{\beta} \left[\frac{1}{\gamma^2(1-\beta \cos\theta)} - 1 \right], \quad (12)$$

and the two sets of coefficients correspond to the initial and final state, respectively. Unless the energy of the incident electron is exceedingly low, the reciprocal-lattice vectors \mathbf{g} are overwhelmed by the wave vector \mathbf{k} and Eq. (11) is reduced to the dipole radiation formula. This is the case for channeling radiation (c.f., Fig. 2). There is little azimuthal variation and little need for a large number of coefficients in the evaluation of the expression in Eq. (11). For high-energy transitions, however, the coefficients involved are such that the behavior near the endpoint of the θ interval is modified. Figure 6 shows this bremsstrahlung intensity for 100-keV electrons in diamond.⁹ The graph corresponds to the first high-energy transition (c.f. Fig. 2). Other transitions of this type behave similarly. For comparison, the dipole radiation intensity is given in a dashed line. We notice how the bremsstrahlung maximum is shifted toward the forward direction. This type of coherent bremsstrahlung has a weak azimuthal variation. In order to produce stable re-

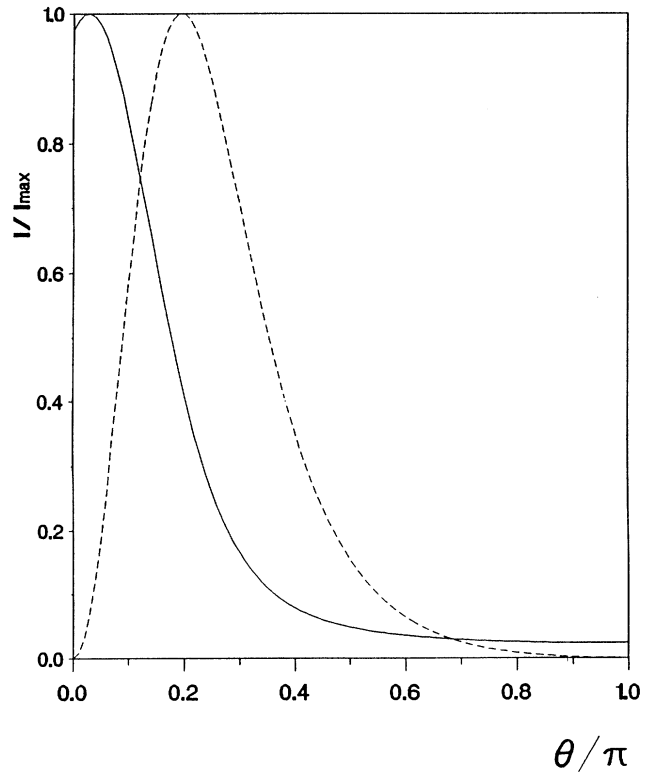


FIG. 6. Angular dependence of the intensity for coherent bremsstrahlung emanating from 100-keV electrons along the $\langle 100 \rangle$ direction in diamond. The corresponding dipole radiation intensity is given in the dashed line.

sults, these calculations may require the use of up to 500 basis functions. We have, once again, disregarded the change in relativistic mass, partly because the effect is marginal but mainly because of the more fundamental approximations (zero-phonon collisions, “pseudopopulation” of states, etc.) underpinning the entire approach. Despite the questionable accuracy of the straightforward quantum-mechanical approach, it still appears to suffice for the analysis of experimental data.^{8,9,20} One may conclude that an accurate quantum-mechanical treatment of

this type of coherent bremsstrahlung ought to include phonons.

ACKNOWLEDGMENTS

The financial support of the Catholic University of America through the National Science Foundation (Contract No. PHY 8911619) is gratefully acknowledged. We wish to thank R. Fusina for helpful discussions.

*Also at the Institute for Theoretical Physics, Chalmers University of Technology, Göteborg, S-41296, Sweden.

†Also at the Naval Research Laboratory, Complex Systems Theory Branch, Washington, D.C., 20375, and SFA Inc., Landover, MD 20785.

¹*Coherent Radiation Sources*, edited by A. W. Sáenz and H. Überall (Springer, Berlin, 1985).

²J. U. Andersen, K. R. Eriksen, and E. Lægsgaard, *Phys. Scr.* **24**, 588 (1981).

³J. U. Andersen, E. Bonderup, E. Lægsgaard, B. B. Marsh, and A. H. Sørensen, *Nucl. Instrum. Methods* **194**, 209 (1982).

⁴J. U. Andersen, S. Datz, E. Lægsgaard, J. P. F. Sellschop, and A. H. Sørensen, *Phys. Rev. Lett.* **49**, 215 (1982).

⁵G. Kurizki, *Phys. Rev. B* **33**, 49 (1986).

⁶G. H. Golub and C. F. van Loan, *Matrix Computations*, 2nd ed. (Johns Hopkins, Baltimore, 1989).

⁷J. K. Cullum and R. A. Willoughby, *Lanczos Algorithms for Large Symmetric Eigenvalue Computations* (Birkhauser, Boston, 1985) Vols. I and II.

⁸J. C. H. Spence, G. Reese, N. Yamamoto, and G. Kurizki, *Philos. Mag. B* **48**, L39 (1983).

⁹G. M. Reese, J. C. H. Spence, and N. Yamamoto, *Philos. Mag. A* **49**, 697 (1984).

¹⁰P. A. Doyle and P. S. Turner, *Acta Crystallogr. A* **24**, 390 (1968).

¹¹S. Datz *et al.*, *Phys. Lett.* **96A**, 314 (1983).

¹²E. Lægsgaard and J. U. Andersen, *Nucl. Instrum. Methods B* **2**, 99 (1984).

¹³P. Lervig, J. Lindhard, and V. Nielsen, *Nucl. Phys. A* **96**, 481 (1967).

¹⁴*Relativistic Channeling*, edited by R. A. Carrigan, Jr. and J. A. Ellison (Plenum, New York, 1987).

¹⁵E. I. Rozum, S. A. Vorob'ev, and V. V. Kaplin, *Dokl. Akad. Nauk SSSR* **310**, 861 (1990) [*Sov. Phys. Dokl.* **35**, 156 (1990)].

¹⁶H. Nitta, *J. Phys. Soc. Jpn.* **59**, 2020 (1990).

¹⁷N. W. Ashcroft and N. D. Mermin, *Solid State Physics* (Holt, Rinehart and Winston, Philadelphia, 1976).

¹⁸J. U. Andersen, E. Bonderup, E. Lægsgaard, and A. H. Sørensen, *Phys. Scr.* **28**, 308 (1983).

¹⁹C. Itzykson and J.-C. Zuber, *Quantum Field Theory* (McGraw-Hill, New York, 1980).

²⁰G. Kurizki and J. K. McIver, *Phys. Rev. B* **32**, 4358 (1985).